XLIII CILAMCE
21–25, November, 2022
FOZ DO IGUAÇU – PR – BRAZIL

Post-cracking behavior in tensile for UHPFRC using inverse analysis, fracture energy and finite element method

R. Rojas[1], J. R. Yepez[1]

[1]Engineering School, Federal University of Rio Grande
Italy Avenue, 96203-900, RS/Rio Grande, Brazil
r.rojas@furg.br, j.yepez@furg.br

Abstract. Ultra-high performance fiber reinforced concrete (UHPFRC) is an advanced composite material characterized by compressive and tensile strengths above 150MPa and 7MPa, respectively. Initially, an experimental procedure was used to characterize the tensile performance through bending tests, using beams with 1% and 2% content by volume of steel fibers. Three-point bending load arrangement notched prisms were used to determine the contribution of the fibers to reinforcing a cracked section. With that, the (F vs. ω) experimental curves were graphed, and from there, the analytic tensile curves (σ vs. ω) was obtained point by point by application of the inverse analysis procedure proposed by the AFGC. With the analytic curves, the fracture energy was calculated, following a procedure proposed by RILEM. Subsequently, the crack width was transformed into strain using a relationship that involves the characteristic length. The resulting analytical behavior law was used to carry out computational modeling applying the finite element method. Both the finite element method and the fracture energy were used to validate the procedures, comparing experimental and numerical results. Models and experiments showed good agreement and finally was determined the constitutive law for the UHPFRC in tension. It can be concluded from this study, therefore, that the post-cracking tensile behaviour of UHPFRC can be appropriately evaluated and validated through the applied analysis procedure in this research.

Keywords: experimental tensile test, finite element method, fracture energy, inverse analysis, UHPFRC.

1 Introduction

In this work, UHPFRC beams with steel fiber content by volume of 1% and 2% were subjected to three-point bending tests in the lab. Their responses, in terms of load vs. deflection (F vs. δ), were recorded and showed herein graphically. From there, the analytic tensile curves (σ vs. ω) was obtained point by point by application of the inverse analysis procedure proposed by the Association Française de Génie Civil, AFGC [1]. With the analytic curves, the fracture energy was calculated, following a procedure proposed by the International Union of Laboratories and Experts in Construction Materials, Systems and Structures, RILEM [2]. The crack width was transformed into strain using a relationship that involves the characteristic length. The resulting analytical behaviour law was used to carry out computational modeling applying the finite element method. The program ANSYS [3] was used to carry out computational modeling and obtain the analytical load vs. deflection curves. The ANSYS program requires, as input data, the constitutive behavior of the material in compression and in tensile. Both the finite element method and the fracture energy were used to validate the procedures, comparing experimental and numerical results.

2 Experimental program

The mixture design used in this study is observed in Table 1, it shows the proportions of the mixture, in which 26% of the cement is replaced by sustainable materials. Ground Granulated Blast Furnace Slag (GGBS) and commercial silica fume (SF) are agglomerating sustainable materials used in the mixture. It has a single aggregate

consisting of silica sand with a maximum grain size of 0.30 mm. A solution of polycarboxylate is used as a super-plasticizer additive, which adjusts the workability of the concrete. The fiber used is of the steel, 13 mm long and 0.2 mm in diameter. The water/cement ratio is 0.19 and the water/binder ratio is 0.13.

Table 1: UHPFRC mix design.

Material	kg/m³
Cement	955
GGBS	263
Silica Fume	119
Quartz powder	119
Fine sand	788
Superplasticizer	40
Water	185

Three-point bending load arrangement notched prisms were used to determine the contribution of the fibers to reinforcing a cracked section. With that, the (F vs. ω) experimental curves were graphed. Ten beams (four with 1% of fiber content and six with 2%), were manufactured with the mix presented in Table 1 and with the dimensions of 10x10x40cm. The lab tests were carried out in a hydraulic universal testing machine with a capacity of 2000kN, after 28 days of curing and by applying displacements at a speed of 0.5mm/min. All of them had a notch of 30mm in depth by 4mm in width at the bottom centre of their span length made with a circular saw. A horizontal LVDT type sensor was placed to measure the opening of the notch (ω) and two vertical LVDTs, placed on each side of the beams, were used to measure their central deflection (δ).

3 Analytical investigation

The procedure to determine the constitutive law for the UHPFRC in tension, including the post-cracking response, followed the methodology by AFGC [1]. The tensile curve was obtained point by point by application of the Inverse Analysis, i.e., obtaining the σ vs. ε analytic curve from the F vs. ω experimental curve. Both curves σ vs. ε in compression and in tension were introduced as input data for the computational modeling and then the F vs. δ analytical curve was obtained. Therefore, a graphical comparison between the experimental and the analytical behaviors for each of the specimens tested were carried out.

3.1 Inverse analysis

The process starts with the definition of a new coordinate system at the point where the first crack occurs. The notch opening value at that point is turned into the new origin, with the first point coinciding with the elastic limit. The equilibrium is easily solved to find the internal force. From the first point (step i), the next points are calculated (steps i+1) by solving the equilibrium of the cracked section. A complex nonlinear equation system is generated at each step and, therefore, the free software Máxima [4] was used as a mathematical tool to solve the equations. After, the tension at the point is calculated, i.e., in this case, the cohesive tension.

The process is repeated at each i+1 point until the curve of cohesive tension versus notch opening is built (actually, the σc vs. ω curve). Then, the σc vs. ω curve is transformed into a σ vs. ε curve, which, according to AFGC [1], can be used to define a relation between ω and ε mainly based in a determination of the characteristic length (lc), see eq. (1). The characteristic length is measured at the location where cracking occurs and in the same direction of the bottom notch opening of the beam. In the case beams are subjected to three-point bending, the AFGC [1] defines the lc value as a function of the type of experimental behavior that is presented, i.e., the value depends upon the behavior as either of the strain softening or strain hardening types. If the beam presents a strain softening type of behavior, the characteristic length is calculated with eq. (2), while if presenting a strain hardening behavior, eq. (3) is therefore used.

$$\varepsilon = \frac{\mathrm{fct,el}}{\mathrm{E}} + \frac{\omega}{\mathrm{lc}}. \tag{1}$$

$$lc = \frac{2\,(h - a)}{3}. \tag{2}$$

$$lc = \frac{E \cdot G_F}{fst^2}. \tag{3}$$

The notation adopted is as follows: fct,el is the tensile strength of the concrete matrix; E is the modulus of elasticity of the concrete matrix; lc is the characteristic length; ω is the notch opening; fst is the direct tension strength; a, h are the notch depth and the beam height, respectively; and G_F is the fracture energy.

3.2 Finite element method (FEM)

The computational analysis was carried out with software ANSYS [4] and choosing its element SOLID185 to model the concrete in 3D. After the concrete experiences a cracking phase, the internal forces are transmitted to the fibers, which then govern the behavior of the material. The Multilinear Material Model used in this work (CAST) can approximate behavior laws both in compression and in tension. Fig. 1 describes the boundary conditions of the beam considered in the model.

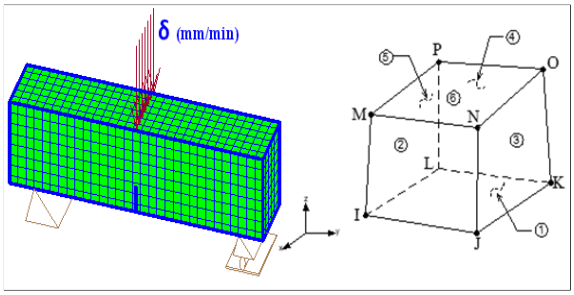

Figure 1. Boundary element and element SOLID 185

The UHPFRC was simulated as a composed material with a law in compression that was obtained from experimental data and a law in tension from an Inverse Analysis that includes the material's post-cracking behavior. SOLID185 is a 3D element that allows considerations to represent plasticity, hyperelasticity, large displacements, and large strains. It also allows simulations of quasi-incompressible elastoplastic materials and fully incompressible hyperelastic materials. The element is defined by eight nodes with three degrees of freedom each (translations in x, y, and z directions), as shown in Fig. 1. CAST is an elastic isotropic multilinear material with the same elastic behavior in compression and in tension, but with elastic limit and isotropic hardening behavior that can be different in each case.

The behavior in tension uses the Rankine criterion, while the behavior in compression uses Von Mises. The UHPFRC properties, such as its modulus of elasticity and its Poisson's coefficient, had to be known for the simulations. These values were maintained constant in each specimen that was modeled. The behavior laws in tension and in compression were different in each specimen since those behaviors were drawn from the experimental tests and the results from the Inverse Analysis.

3.3 Forces in cracked section

Figure 2 shows the cracked cross-section of a prismatic beam subjected to bending forces, and where two different regions can be easily identified. Firstly, there is the zone without any cracking, which is the part of the section where the force distribution corresponds to a linear elastic behavior. Secondly, there is the cracked zone, which is the part of the section where the force distribution directly depends on the effectively of the fibers inside the concrete matrix, which can be determined via Inverse Analysis.

The force equilibrium in the section results in eq. (4) to eq. (8) with "b" identifying the contribution of the regions with cracks, while "f" identifies the cracked ones. The system of eight equations to solve is bound to eq. (9) to eq. (16), shown in the following. The equation system is solved for each point of the (σ vs. ω) curve by using

the known experimental points (F vs. ω) and the parameters calculated in the previous step.

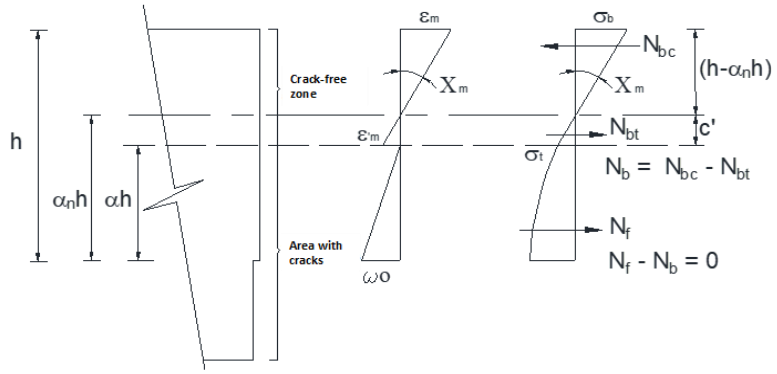

Figure 2. Forces in the cracked section. AFGC [1] modified

$$\mathrm{Nbc} = \frac{1}{2} \cdot \sigma\mathrm{b} \cdot \mathrm{c} \cdot \mathrm{b}. \tag{4}$$

$$\mathrm{Nbt} = \frac{1}{2} \cdot \sigma\mathrm{t} \cdot c' \cdot \mathrm{b}. \tag{5}$$

$$\mathrm{Nb} = \mathrm{Nbc} + \mathrm{Nbt}. \tag{6}$$

$$\mathrm{M} = \mathrm{Mb} + \mathrm{Mf}. \tag{7}$$

$$\mathrm{N} = \mathrm{Nb} + \mathrm{Nf}. \tag{8}$$

$$\mathrm{Nb} = \frac{1}{2} \cdot \mathrm{E} \cdot \mathrm{Xm} \cdot \mathrm{b} \cdot \mathrm{h}^2 \cdot [A^2 - B^2]. \tag{9}$$

$$\mathrm{Nf_{i+1}} = \mathrm{Nf_i} \cdot \mathrm{C} \cdot \mathrm{D} + \mathrm{K} \cdot \mathrm{b} \cdot \mathrm{H} \cdot (1 - D). \tag{10}$$

$$\mathrm{Mb} = \frac{1}{3} \cdot \mathrm{E} \cdot \mathrm{Xm} \cdot \mathrm{b} \cdot \mathrm{h}^3 \cdot [A^3 - B^3] + \mathrm{h} \cdot \alpha\mathrm{n} \cdot \mathrm{Nb}. \tag{11}$$

$$\mathrm{Mf_{i+1}} = \mathrm{Mf_i} \cdot (\mathrm{C}.\mathrm{D})^2 + K \cdot \mathrm{Nf_{i+1}} \cdot \mathrm{O} - \mathrm{L} \cdot O^2 \sigma\mathrm{f_{i+1}}. \tag{12}$$

$$\mathrm{N} = \mathrm{Next} = \mathrm{Nb} + \mathrm{Nf}. \tag{13}$$

$$\mathrm{M} = \mathrm{Mext} = \mathrm{Mb} + \mathrm{Mf}. \tag{14}$$

$$\sigma\mathrm{t} = \mathrm{E} \cdot \mathrm{Xm} \cdot \mathrm{h} \cdot (\alpha\mathrm{n} - \alpha). \tag{15}$$

$$\omega = \left[Xm + 2 \cdot \frac{M}{E \cdot I}\right] \cdot \frac{2\,(\alpha \cdot h)^2}{3}. \tag{16}$$

The notation adopted is as follows: h.α is the relative length of the crack; h.αn is the relative height of the neutral axis; Xm is the curvature of the region without cracks; b, h are the width and height of the beam cross-section, respectively; I is the moment of inertia of the rectangular section; and the variables are:

$\mathrm{A} = 1 - \propto_{\mathrm{n}}$; $\mathrm{B} = \propto - \propto_{\mathrm{n}}$; $\mathrm{C} = \frac{\propto_{\mathrm{i+1}}}{\propto_{\mathrm{I}}}$; $D = \frac{\omega_i}{\omega_{i+1}}$; $H = \frac{\sigma f_i + \sigma f_{i+1}}{2}$; $K = \alpha_{\mathrm{i+1}}.\mathrm{h}$; $L = \frac{(\alpha_{\mathrm{i+1}}.\ \mathrm{H})^2\ .\mathrm{b}}{2}$; $O = 1 - D$

3.4 Validation using energy fracture and finite element method

The area under the analytical (σ vs. ω) curve, which is obtained via the Inverse Analysis commented in the previous section, represents the fracture energy, G_F, of the material. In the same form, the area under the experimental (F vs. δ) curve gives a measure of G_F, calculated according to specifications given by RILEM TC50 [3]. The Fracture Energy can be found using the load-displacement data and the eq. (17). A graphical comparison is made between both behaviors and the fracture energy is then calculated for every specimen with 1% and 2% of fiber content. The notation adopted is as follows: W_f is the total area of the curve under the graphic of load versus deflection; b is the thickness of the beam (mm); h is the height (mm); and a is the length of the notch made in the lower center of the beam.

$$G_F = \frac{W_f}{b \cdot (h - a)}. \tag{17}$$

The law of behavior in compression is obtained from the experimental data, and the law of behavior in tensile is obtained by inverse analysis. The numerical simulation of the flexural test is performed using these behavior curves as input data. An analytical load-displacement curve is obtained for each of the specimens. Then this analytical curve is compared with the response obtained experimentally. The approximation between the analytical and experimental curves, indicated above, is a measure adopted in this investigation to validate the inverse analysis. With this, it is possible to verify the effectiveness of the methodology proposed by the French standard in the AFGC [1], developed from the mechanical equilibrium of Fig. 2 and by eq. (4) to eq. (16).

4 Results

Using the mixture design indicated in Table 1 were tested specimens and the compressive strength was calculated as the average values, resulting in 151MPa. In each test, the σ-ε curve was obtained and the modulus of elasticity, which averaged 48GPa. These parameters were used as input to numerical simulation. The graphics results in tensile, considering fiber content of 1% and 2%, are showed in Fig. 3 and Fig. 4 respectively.

Item a) in the figures shows (F vs. δ) curves for each of the tested beams, as well as the average curve. The area under each curve was calculated to determine the fracture energy according to RILEM TC50 [2] see Table 2. The values of the elastic load, Fte; of the elastic strength in tension, σ; and of the deflection, δte; are presented in Table 3. Also, it presents the results obtained from the post-cracking behavior for the maximum load Ftcr and its corresponding deflection δtcr. Item b) in the figures shows (σ vs. ω) curves obtained from Inverse Analysis for each one of the beams. The area under each relation (σ vs. ω) was calculated to determine the fracture energy, as is showed in Table 2 for each one of the tested specimens, where a good fit can be observed between the two averaged results. Item c) in the figures shows (σ vs. ε) curves obtained from the transformation of ω into ε using eq. (1) to eq. (3). Item d) in the figures shows the results of computational modeling (analytical response) e also the average experimental response, models and experiments showed good agreement.

Table 2. Fracture Energy (GF) for UHPFRC beams with 1% and 2% of fibers

	Fracture Energy (kJ/m²)			
	1% of fibers		2% of fibers	
Specimen	Inverse Analysis AFGC	RILEM TC50-FMC	Inverse Analysis AFGC	RILEM TC50-FMC
CP-1	16.91	11.66	26.53	23.76
CP-2	23.71	18.75	29.29	19.17
CP-3	23.70	15.42	29.19	23.10
CP-4	23.32	19.22	18.87	21.76
CP-5			32.49	32.40
CP-6			32.48	57.96
Average	21.91	16.26	26.67	24.04

Table 3. UHPFRC elastic and inelastic load and deflection, and strength in bending

	Fte (kN)		δte (mm)		σ (MPa)		Ftcr (kN)		δte (mm)	
Specimen	1%	2%	1%	2%	1%	2%	1%	2%	1%	2%
CP-1	9.9	20.0	0.032	0.030	9.1	18.4	9.2	21.0	0.83	0.81
CP-2	10.0	15.1	0.039	0.024	9.2	18.5	11.4	20.8	1.30	1.03
CP-3	10.1	15.1	0.039	0.030	9.3	13.8	13.8	22.5	1.04	1.08
CP-4	10.6	10.3	0.037	0.020	9.7	9.5	14.3	22.0	1.28	1.04
CP-5		10.2		0.018		9.3		23.4		0.91
CP-6		10.3		0.021		9.4		26.4		1.09
Average	10.1	13.5	0.037	0.024	9.3	13.2	12.2	22.7	1.11	0.99

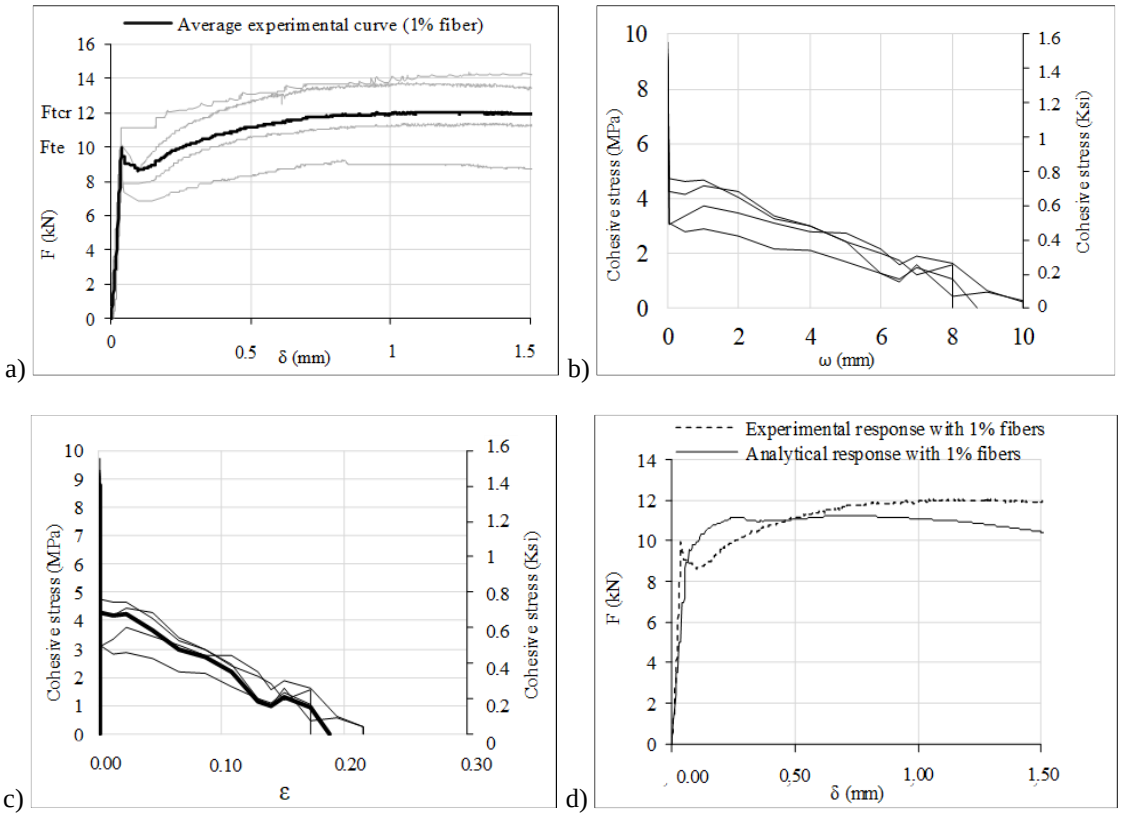

Figure 3. Beams with 1% of fibers in bending: a) Experimental curves; b) Numerical (σ vs. ω) curves; c) Numerical (σ vs. ε) curves; d) Experimental vs. numerical average response

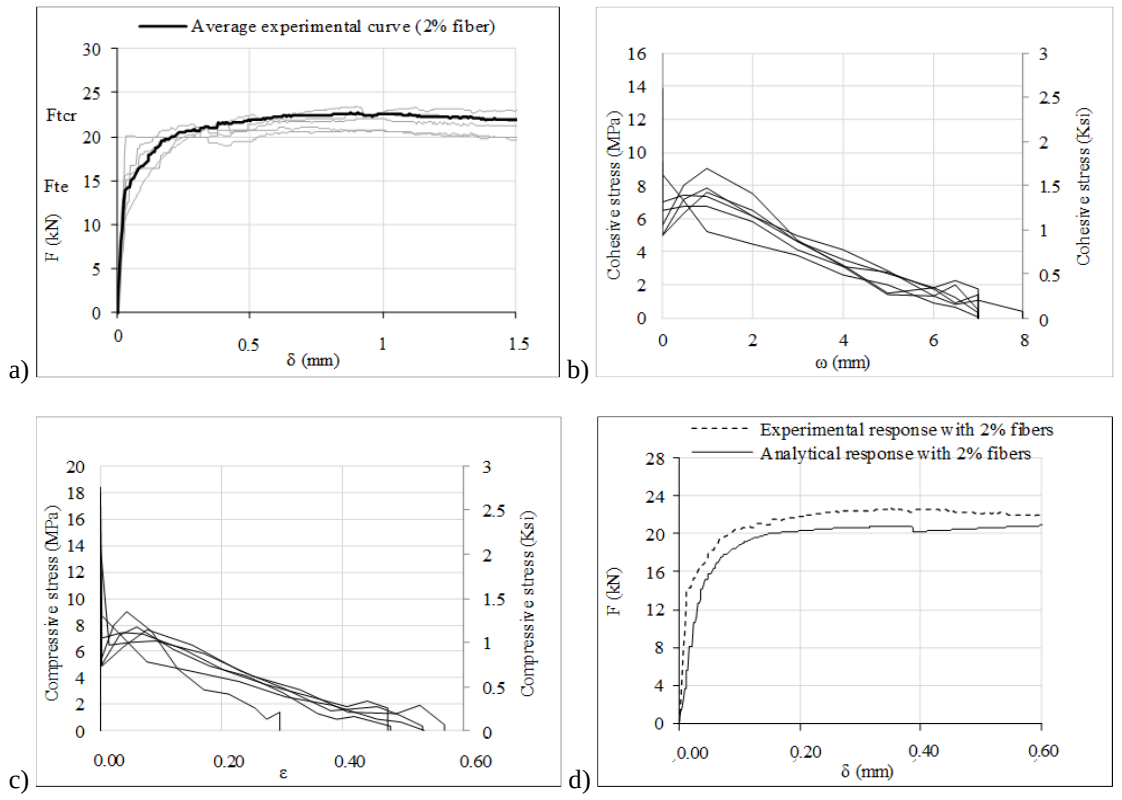

Figure 4. Beams with 2% of fibers in bending: a) Experimental curves; b) Numerical (σ vs. ω) curves; c) Numerical (σ vs. ε) curves; d) Experimental vs. numerical average response

The behavior analytic curves obtained in this research showed a similar trend with the curves (F vs. δ) obtained by Denairé et al. [5] using inverse analysis. Similarly, Mezquida et al. [6] carried out inverse analysis methodologies, based on the closed-form non-linear hinge model, to define the material's behavior. They obtained a similar response to this research in both cases: when the UHPFRC exhibits strain-hardening constitutive stress-strain behavior and when it exhibits strain-softening behavior. Also, Chanvillard and Rigaud [7] studied three points bend test on notched specimens and applied an inverse analysis to extract the tensile strength versus crack opening relationship. Again, the behavior curves showed a similar trend to the results in this research.

5 Conclusions

The computational modeling of UHPFRC beams can be satisfactorily carried out by considering the behavior of the composite material under a homogeneous premise. This can be accomplished with bending tests and the determination of behavior laws for the matrix with fibers in uniaxial compression and tension;

The constitutive laws for the UHPFRC material were experimentally and numerically determined for each of the beams considered. The σ vs. ε curves obtained in each case were considered as input data for the computational modeling carried out in Finite Elements in ANSYS. The results generated numerical F vs. δ curves that were compared with the ones experimentally obtained, showing a good fit between them;

The finite element SOLID185 used to model the matrix, together with the CAST material model used to simulate the behavior of the cracked section governed by fibers, were adequate to model the UHPFRC;

The Inverse Analysis procedure showed to be adequate to determine the behavior curve in tension of the considered beams made of UHPFRC, even considering the post-cracking response of the material;

The validation of the Inverse Analysis by means of calculating the fracture energy showed to be satisfactory for the beams with 2% of fiber content. The average value calculated from (σ vs. ω) numerical curves was 27 kJ/m2, while the value obtained from the experimental (F vs. δ) curves was 24 kJ/m2, i.e., a difference of 10%.

Acknowledgements. The authors acknowledge the financial support given by the Brazilian research agency CAPES as well as the personnel and equipment from the laboratories CEMACOM and LEME of the Graduate Program in Civil Engineering of UFRGS.

Authorship statement. The authors hereby confirm that they are the sole liable persons responsible for the authorship of this work, and that all material that has been herein included as part of the present paper is either the property (and authorship) of the authors, or has the permission of the owners to be included here.

References

[1] ASSOCIATION FRANÇAISE DE GENIE CIVIL. AFGC: Ultra High Performance Fiber Reinforced Concretes. Recommendations. AFGC, 2013.

[2] THE INTERNATIONAL UNION OF LABORATORIES AND EXPERTS IN CONSTRUCTION MATERIALS, SYSTEMS AND STRUCTURES. RILEM. TC50: Determination of Fracture Energy of Mortar and Concrete by means of three-point bend tests on notched beams. *Materials and Structures Journals*, v. 106, n. 18, p. 285-290, 1985. https://www.rilem.net/publication

[3] ANSYS Inc. Engineering Simulation Software. Version 19.2 Canonsburg, c2018.

[4] MAXIMA FREE SOFTWARE. wxMaxima version 17.10.1

[5] Denairé E., Sofia L., Brühwiler E. (2017). "Characterization of the tensile response of strain hardening UHPFRC-Chillon Viaducts". *AFGC-ACI-fib-RILEM International Symposium on UHPFRC*. Montpellier, France.

[6] Mezquida E.; Navarro J. and Serna P. (2019). "Numerical validations Numerical validation of a simplified inverse analysis method to characterize the tensile properties in strain-softening UHPFRC". *Materials Science and Engineering*, n. 596.

[7] Chanvillard G. and Rigaud S. (2003). Complete characterization of tensile proprieties of Ductal UHPFRC according to the french recommendations. In: HPFRCC, RILEM Proceedings Workshop, 2003, Ann Arbor, USA.